

Supporting Information for

Temperature Response of Aqueous  
Solutions of a Series of Pyrene End-Labeled  
Poly(*N*-isopropylacrylamide)s Probed by  
Turbidimetry, Light Scattering, and  
Fluorescence

Mike Fowler<sup>a</sup>, Jean Duhamel\*<sup>a</sup>

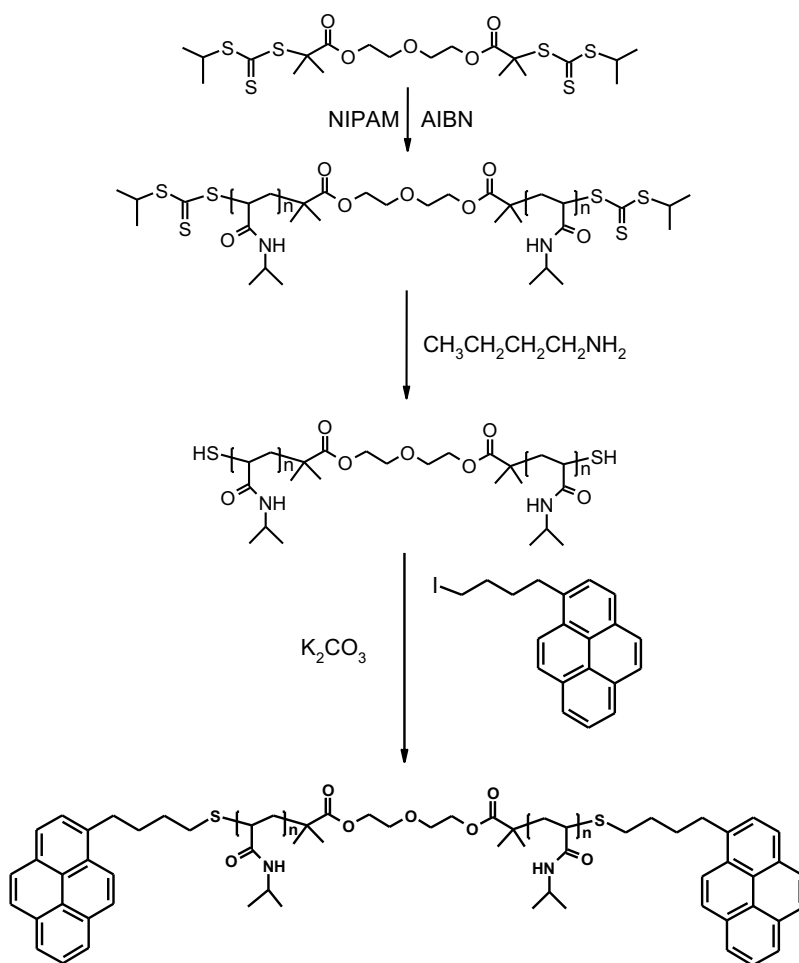
<sup>a</sup> Institute for Polymer Research, Waterloo Institute for Nanotechnology, Department of  
Chemistry, University of Waterloo, Waterloo, ON N2L 3G1, Canada

Xing Ping Qiu<sup>b</sup>, Evgeniya Korchagina,<sup>b</sup> Françoise Winnik\*<sup>b</sup>

<sup>b</sup> Faculty of Pharmacy and Department of Chemistry, Université de Montréal, CP 6128  
Succursale Centre Ville, Montréal QC H3C 3J7, Canada

## Synthesis of the Py<sub>n</sub>-PNIPAM

The preparation and characterization of the Py<sub>n</sub>-PNIPAM samples with  $n = 1$  or 2 have been described in detail earlier.<sup>1,2</sup> The synthesis was carried out according to Scheme S1 for the telechelic Py<sub>2</sub>-PNIPAM samples. The main difference for the synthetic protocol of the telechelic and semi-telechelic Py<sub>n</sub>-PNIPAM samples was the chain transfer agent (CTA). Whereas diethylene glycol di(2-(1-isobutyl)sulfanylthiocarbonyl-2-methylpropionate) (DEGDIM) was employed as a bifunctional CTA for the synthesis of the Py<sub>2</sub>-PNIPAM samples as shown in Scheme S1, the monofunctional CTA ethyl 2-(1-isobutyl)sulfanylthiocarbonyl-2-methylpropionate) was used for the synthesis of the Py<sub>1</sub>-PNIPAM samples.



**Scheme S1.** Synthetic procedure for telechelic Py<sub>2</sub>-PNIPAM.

The distribution of absolute molecular weight of the Py<sub>n</sub>-PNIPAM samples was determined with a GPC instrument equipped with a multi angle laser light scattering (MALLS) detector. Table S1 presents the number average molecular weight ( $M_n$ ) and polydispersity index ( $M_w/M_n$ ) where  $M_w$  is the weight average molecular weight of the polymer. Figure S1 shows all the GPC traces obtained with the polymers.

**Table S1.** GPC-MALLS characterization of the telechelic  $\alpha,\omega$ -di-[4-(1-pyrenyl)butyl] poly(*N*-isopropylacrylamides) (Py<sub>2</sub>-PNIPAM) and semi-telechelic  $\alpha$ -ethyl- $\omega$ -[4-(1-pyrenyl)butyl] poly(*N*-isopropylacrylamides) (Py<sub>1</sub>-PNIPAM) samples

Polymer Sample	$M_n$ (kDa)	$M_w/M_n$
Py <sub>2</sub> -PNIPAM(7K)	7.6	1.08
Py <sub>2</sub> -PNIPAM(14K)	13.7	1.10
Py <sub>2</sub> -PNIPAM(25K)	25.4	1.07
Py <sub>2</sub> -PNIPAM(45K)	44.5	1.10
Py <sub>1</sub> -PNIPAM(7K)	7.7	1.02
Py <sub>1</sub> -PNIPAM(12K)	12.3	1.02
Py <sub>1</sub> -PNIPAM(25K)	23.5	1.09

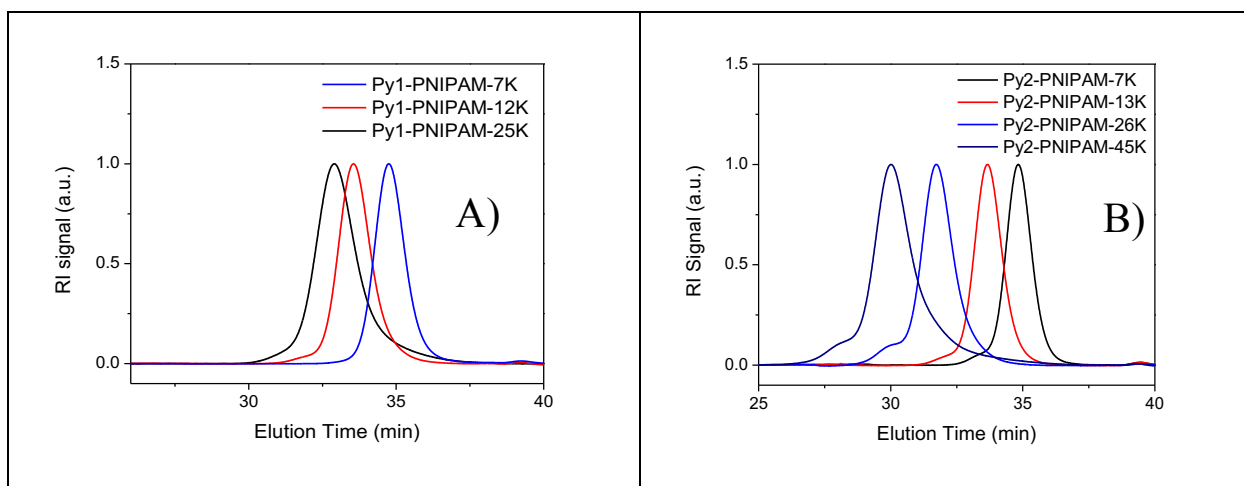


**Figure S1.** GPC-traces of A) semi-telechelic  $\text{Py}_1$ -PNIPAM(7K),  $\text{Py}_1$ -PNIPAM(12K) and  $\text{Py}_1$ -PNIPAM(25K) and B)  $\text{Py}_2$ -PNIPAM(7K),  $\text{Py}_2$ -PNIPAM(13K),  $\text{Py}_2$ -PNIPAM(25K) and  $\text{Py}_2$ -PNIPAM(45K) in DMF at 40 °C.

### Determination of $T_c$ by Turbidimetry

The % transmittance of a 0.5 g/L solution of  $\text{Py}_2$ -PNIPAM(14K) was obtained as a function of temperature with a heating rate of 0.5 °C/min, as shown in Figure S2A. The derivative of the % transmittance was taken, which is shown in Figure S2B.

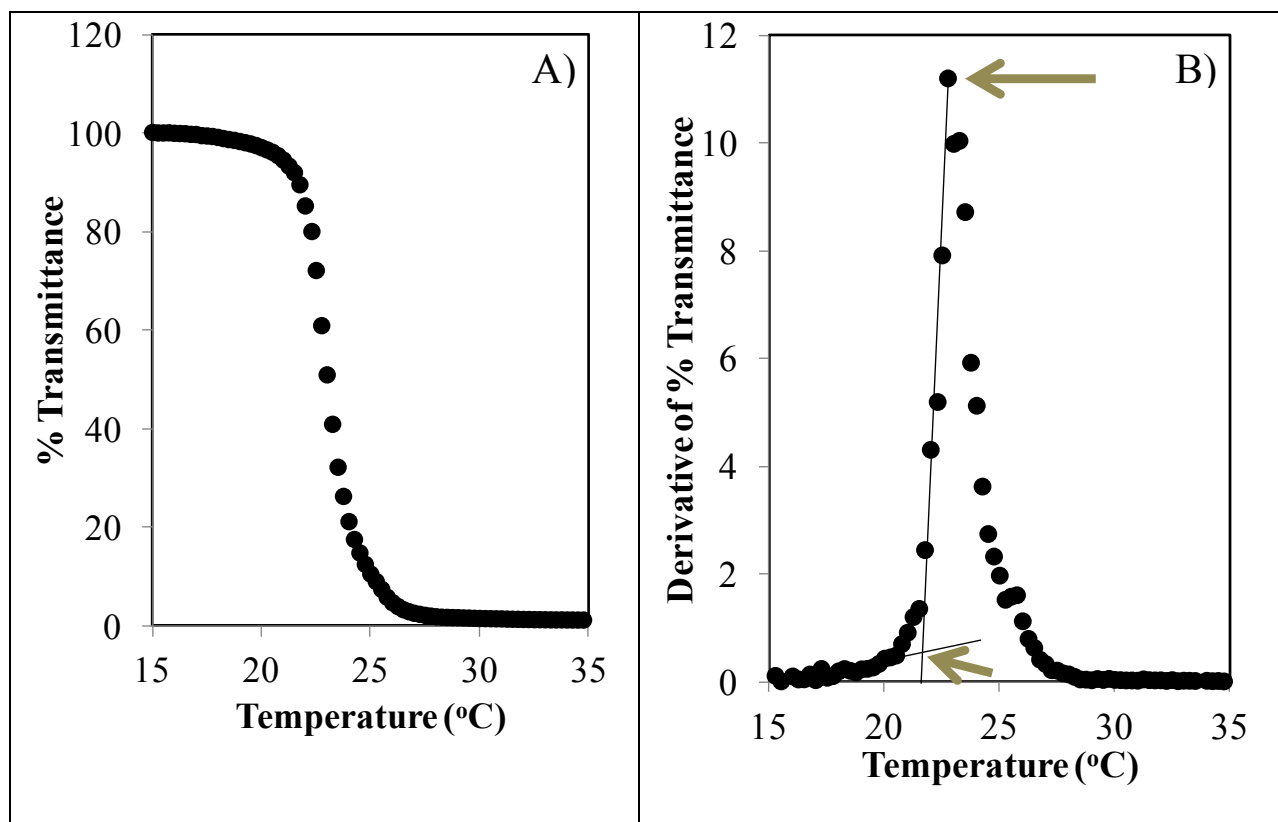


**Figure S2:** Turbidimetry results obtained for 0.5 g/L Py<sub>2</sub>-PNIPAM(14K) with a heating rate of 0.5 °C/min. A) % transmittance curve. B) Derivative curve.

The turbidity curve shown in Figure S3A shows a clear transition from high to low transmittance that occurs over a range of temperature values. When the derivative of the curve is taken, as shown in Figure S2B, the critical temperature could be taken as either the peak in the derivative or the intersection point between the baseline and the rise of the derivative.

The  $T_c$  trends observed for 0.5 g/L solutions with a 0.5 °C/min heating rate are reported in the main text in Figure 3B where  $T_c$  was taken as the derivative onset. The trends for these same solutions where  $T_c$  was taken as the derivative peak are shown in Figure S3.

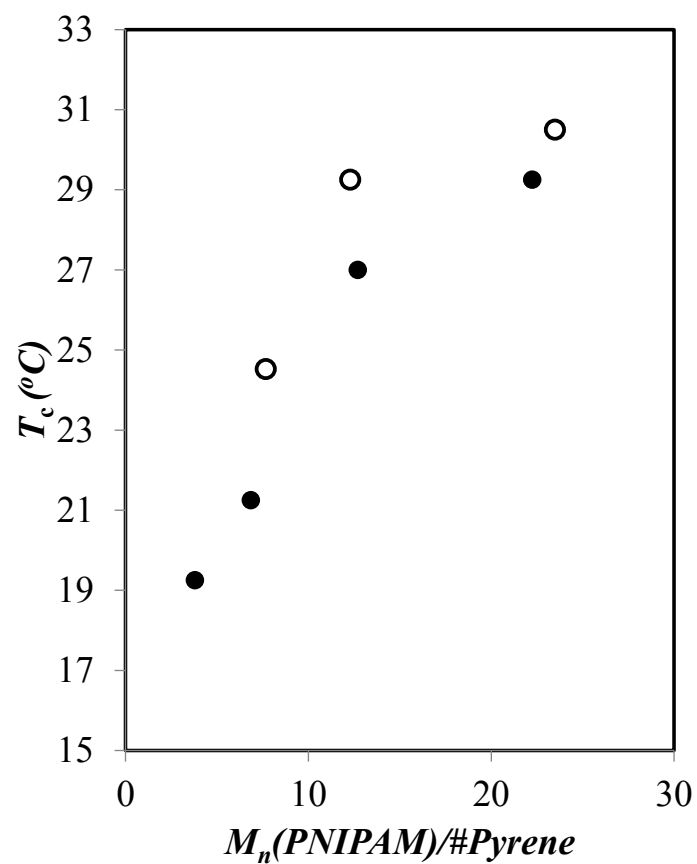


**Figure S3:**  $T_c$  determined from the derivative peak as a function of the ratio of  $M_n$  for the Py-PNIPAM samples over their respective number of pyrenes. (●) Py<sub>2</sub>-PNIPAM (○) Py<sub>1</sub>-PNIPAM

## Analysis of the Fluorescence Spectra

Even at the low polymer concentrations used in the fluorescence experiments, the fluorescence spectra of the Py<sub>2</sub>-PNIPAM solutions showed some light scattering distortion at 350 nm where pyrene does not emit. This is illustrated in Figure S4A that shows the fluorescence spectrum of Py<sub>2</sub>-PNIPAM(14K) at  $T = 26\text{ }^{\circ}\text{C}$  ( $T_c = 24\text{ }^{\circ}\text{C}$  for Py<sub>2</sub>-PNIPAM(14K) obtained from the  $I_E/I_M$  trend in Figure 4. Consequently the analysis of the fluorescence spectra of the doubly labelled PNIPAM samples (Figure S4A) was performed by first applying a light scattering correction. A fluorescence spectrum was acquired for non-fluorescent PNIPAM(22K) above its  $T_c$  to obtain the scattering envelop. It was normalized to the scattering intensity observed in the fluorescence spectrum between 350 and 360 nm, and the normalized scattering envelop was subtracted from the fluorescence spectrum of Py<sub>2</sub>-PNIPAM(14K) to yield the fluorescence spectrum S3C. Then the fluorescence of the pyrene excimer was determined by subtracting the fluorescence spectrum of Py<sub>1</sub>-PNIPAM(25K) at a given temperature normalized to the fluorescence intensity at 375 nm of the Py<sub>2</sub>-PNIPAM(14K) sample. Py<sub>1</sub>-PNIPAM(25K) showed hardly any excimer over the entire temperature range and was used as a model representative of the pyrene monomer. The spectra of Py<sub>1</sub>-PNIPAM(25K) were employed to carry out the subtraction. After subtraction, the fluorescence spectrum shown in Figure S4D was obtained. The “spiky” features observed in the 370 – 390 nm range in Figure S4C are the result of a slight mismatch between the wavelengths in the fluorescence spectra of the pyrene monomer for the Py<sub>1</sub>-PNIPAM(25K) and the corresponding Py<sub>2</sub>-PNIPAM sample. The fluorescence spectrum of the excimer shown in Figure S4D was then integrated from 420 to 600 to yield  $I_E$  in the  $I_E/I_M$  calculations.

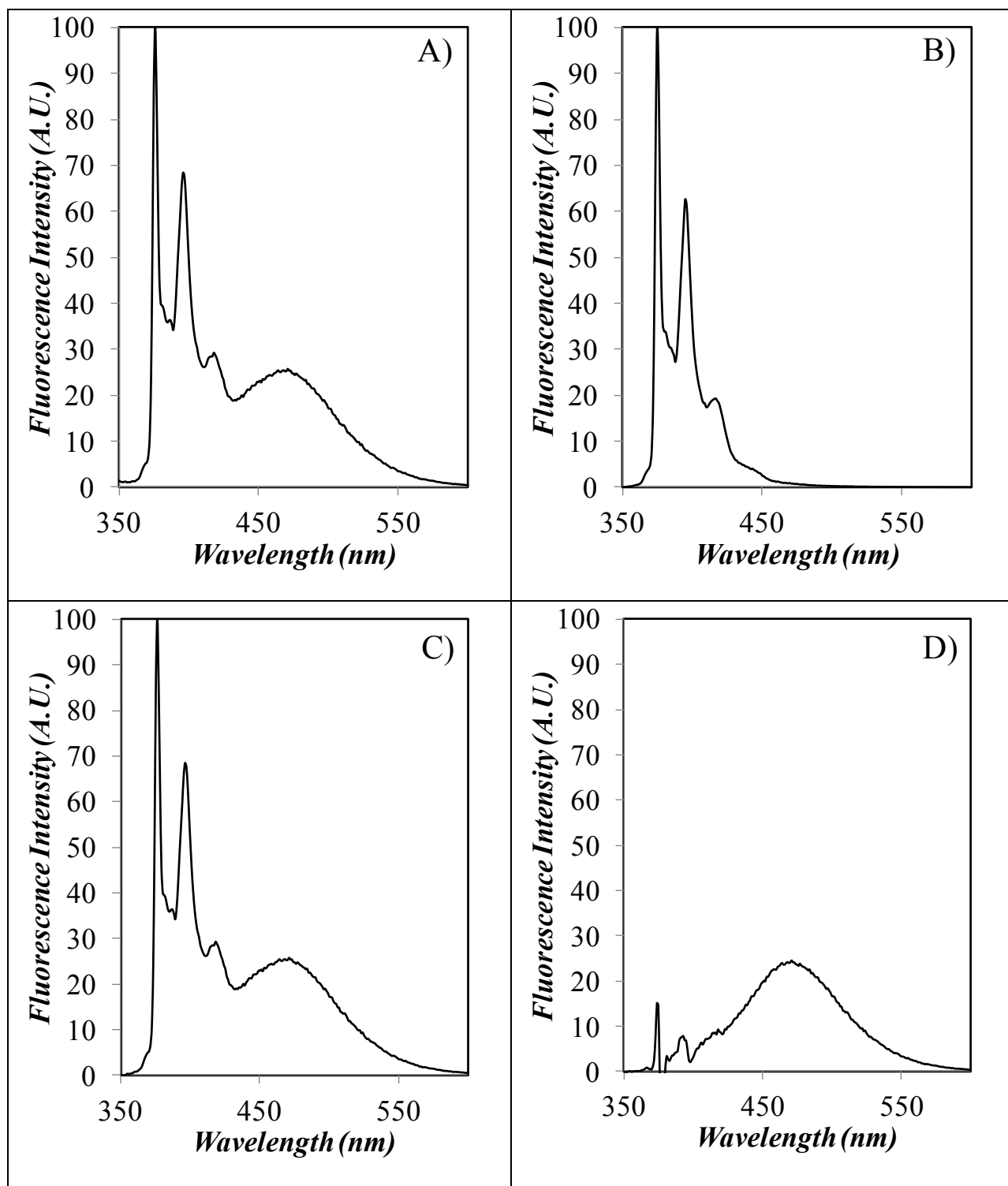


**Figure S4:** Representative fluorescence spectra of Py<sub>2</sub>-PNIPAM(14K) at 26 °C. A) Uncorrected fluorescence spectrum. B) Monomer fluorescence spectrum. C) Spectrum after the application of a light scattering correction. D) Spectrum after subtraction of the monomer fluorescence.



## Example Fluorescence spectra and decays

Time resolved fluorescence decays and steady-state fluorescence spectra were acquired for the aqueous  $\text{Py}_n$ -PNIPAM solutions, examples of which are shown in Figure S5.

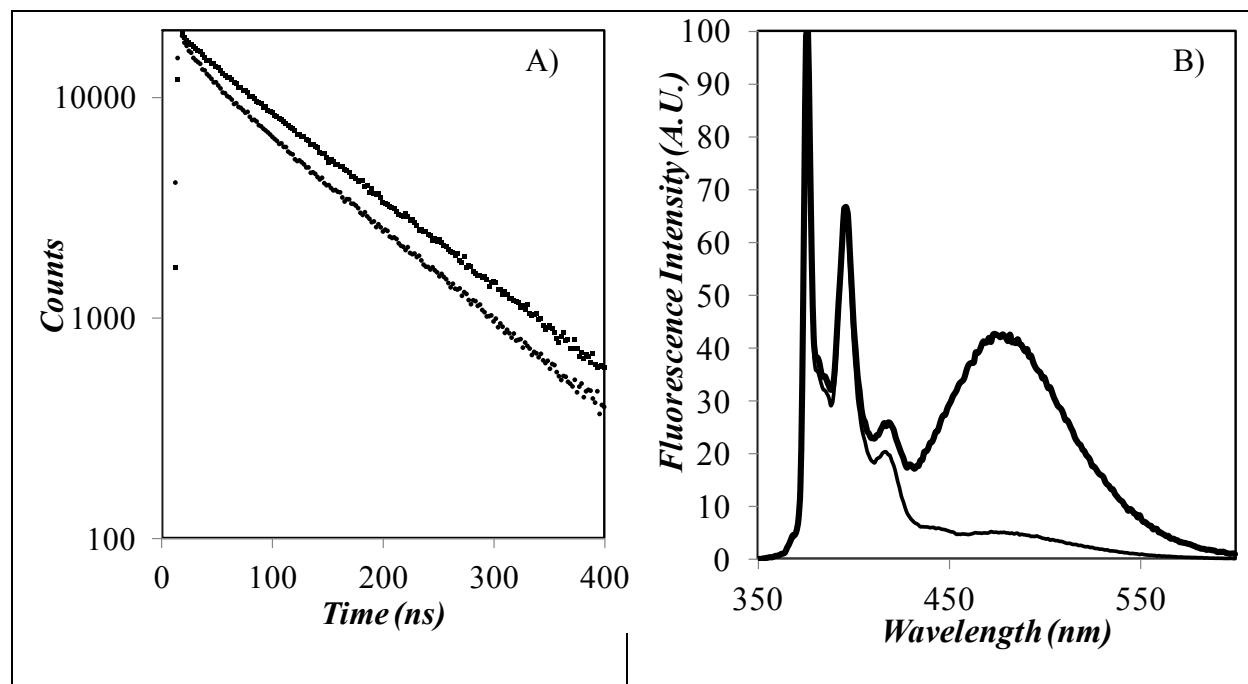


**Figure S5.** Pyrene monomer fluorescence decays and steady-state emission spectra. A) Upper decay:  $\text{Py}_2$ -PNIPAM(14K). Lower decay:  $\text{Py}_2$ -PNIPAM(25K) B) Upper Spectrum:  $\text{Py}_2$ -PNIPAM(14K). Lower spectrum:  $\text{Py}_2$ -PNIPAM(25K)

## $T_c$ measured by DLS.

The increase in turbidity of the aqueous  $\text{Py}_n$ -PNIPAM solutions observed as a function of temperature was due to an increase in the amount of light being scattered by the solution as a result of an increase in the size of the particles being generated in solution. To determine the exact nature of the changes in particle size, dynamic light scattering (DLS) measurements were carried out as a function of temperature for the  $\text{Py}_n$ -PNIPAM aqueous solutions, the results of which are shown in Figure S6.

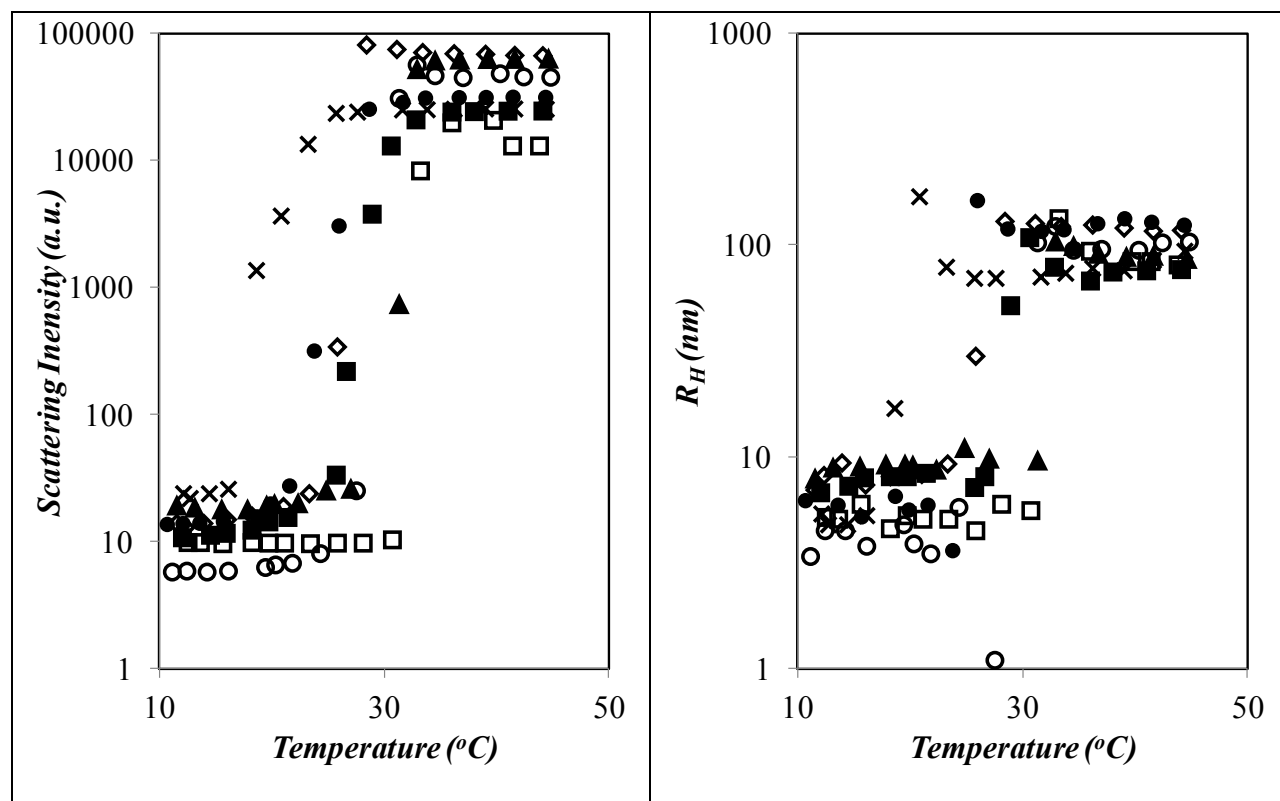


**Figure S7:** DLS measurements for Py-PNIPAM as a function of temperature A) Intensity of scattered light. B) Hydrodynamic radius. (x) Py<sub>2</sub>-PNIPAM(7K), (●) Py<sub>2</sub>-PNIPAM(14K), (■) Py<sub>2</sub>-PNIPAM(25K), (▲) Py<sub>2</sub>-PNIPAM(45K), (◇) Py<sub>1</sub>-PNIPAM(7K), (○) Py<sub>1</sub>-PNIPAM(12K), and (□) Py<sub>1</sub>-PNIPAM(25K).

The light scattering intensity profiles shown in Figure S6A undergo a sharp transition at temperatures corresponding to the cloud point of the respective Py<sub>n</sub>-PNIPAM solutions. The size of the objects present in each solution increased significantly at  $T_c$ , indicating the formation of mesoglobules (Figure S6B). Interestingly, the temperature at which this size transition took place for the Py<sub>1</sub>-PNIPAM solutions matched the temperature of the Py<sub>2</sub>-PNIPAM solutions with the same pyrene content and polymer concentration, and both trends agreed remarkably well with the values of  $T_c$  determined by turbidimetry (Figure 1B). The polymer coil size of the Py<sub>n</sub>-PNIPAM

samples in solution, as determined from the DLS measurements, was then compared to the theoretically derived hydrodynamic radii for single chains in Table 2 (see Grosberg, A. Y.; Kokhlov, A. R. *Statistical Physics of Macromolecules*. American Institute of Physics Press: New York, 1994).

While the theoretical determination neglected the presence of the pyrene moieties, the theoretical hydrodynamic radius ( $R_H$ ) for the longer semi-telechelic Py<sub>1</sub>-PNIPAM(12K) and Py<sub>1</sub>-PNIPAM(25K) chains showed a relatively good agreement with the experimental  $R_H$  values measured by DLS. This observation led to the conclusion that the longer, and thus more hydrophilic, semi-telechelic chains exist primarily as unimers in solution. In contrast, the theoretical  $R_H$  values for the Py<sub>2</sub>-PNIPAM samples were all significantly smaller than the  $R_H$  values calculated for unimers, leading to the conclusion that these chains exist primarily as micelles in solution.

### **Effect of Polymer Concentration and Heating Rate on $T_c$**

The difficulty in determining  $T_c$  at low concentration and for short chains was due in part to a broadening of the transition whose half point in the transmission profile shifted to higher temperature. This broadening is reflected by the full-width at half-maximum values (FWHM) reported in Tables S2 and S3, which are distinctly larger for the shorter chains and lower polymer concentrations. This represents a problem when conducting turbidimetry measurements with a spectrophotometer to assess the exact temperature of a cloud point as the transition occurring at  $T_c$  decreases in intensity and broadens substantially with decreasing polymer concentration. The breadth of the transition is also significant as it determines the difference between the onset and the mid-point of the change in turbidimetry, as reflected by the onset and peak in the derivative of

the % transmittance. The onset of the change in the derivative of the turbidity of the solution will reflect the behaviour of the least soluble chains; in the case of  $\text{Py}_n$ -PNIPAM these would be the shortest chains. The peak in the derivative will reflect the point at which aggregation is 50% complete, so long as the turbidity above  $T_c$  does not reach zero. It is therefore possible that while the peak in derivative best reflects the behaviour of the solution as a whole, the onset will show the best agreement with light scattering techniques that also are most sensitive to the least-soluble chains.

The effect of the heating rate on  $T_c$  is shown in Figure S7B where  $T_c$  is found to increase with increasing heating rate. This trend reflects the time needed to develop a sufficient number of sticky contacts between different PNIPAM chains to induce mesoglobule formation. By decreasing the heating rate to afford a longer time for interpolymeric contacts to occur, the cloud point of the solution is being detected at a lower temperature. The  $\text{Py}_n$ -PNIPAM(7K) samples also showed distinctly larger FWHM values, regardless of heating rate. The observations made for Figures S7A and B illustrate the difficulty associated with the comparison of trends obtained under different experimental conditions. The  $T_c$  values obtained as a function of heating rate and polymer concentrations have been listed in Tables S4-7.

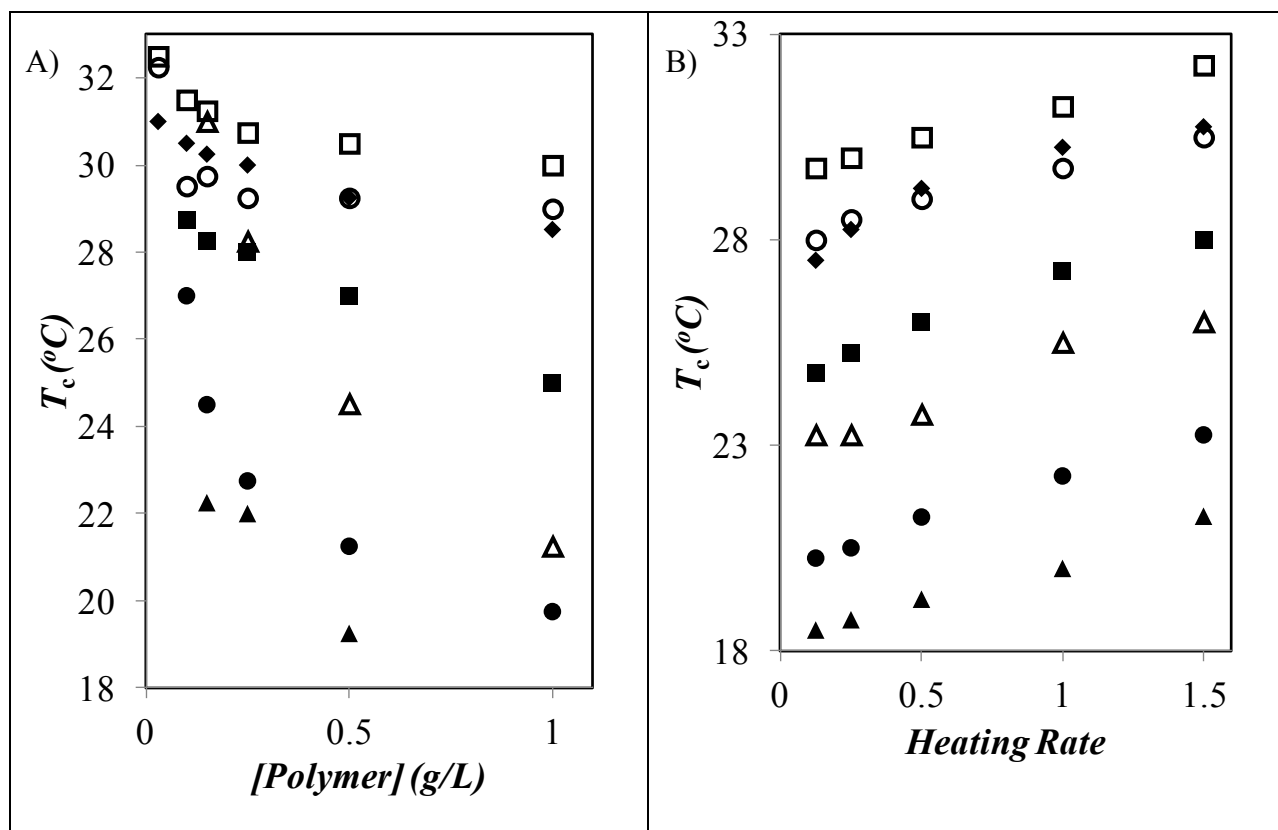


**Figure S7:** Turbidimetry measurements for pyrene-labeled PNIPAM samples as a function of A) polymer concentration with a heating rate of 0.5 °C/min and B) heating rate with a polymer concentration of 0.5 g/L. (▲) Py<sub>2</sub>-PNIPAM(7K), (●) Py<sub>2</sub>-PNIPAM(14K), (■) Py<sub>2</sub>-PNIPAM(25K), (◆) Py<sub>2</sub>-PNIPAM(45K), (△) Py<sub>1</sub>-PNIPAM(7K), (○) Py<sub>1</sub>-PNIPAM(14K), and (□) Py<sub>1</sub>-PNIPAM(25K).

## Turbidimetry Full-Width Half-Max

The Full-Width at Half-Maximum (FWHM) values obtained from the derivative of the transmittance for the Py<sub>n</sub>-PNIPAM solutions are shown in Table S2 and Table S3 for varying concentration and heating-rate, respectively.

**Table S2:** FWHM (°C) of the derivative of the transmittance for Py<sub>n</sub>-PNIPAM solutions with a heating rate of 0.5 °C/min.

[Polymer] (g/L)	Py <sub>1</sub> - PNIPAM (7K)	Py <sub>1</sub> - PNIPAM (12K)	Py <sub>1</sub> - PNIPAM (25K)	Py <sub>2</sub> - PNIPAM (7K)	Py <sub>2</sub> - PNIPAM (14K)	Py <sub>2</sub> - PNIPAM (26K)	Py <sub>2</sub> - PNIPAM (45K)
1.0		1	0.75		2.5	2	1
0.5	7	1	1	1.25	1.75	1.5	1
0.25	5.25	2.25	1.5	3	2.75	1.25	1.5
0.15	4.25	2.75	1.25	4.25	1.5	1.25	1.5
0.1		2.5	1.5			1.25	1.5
0.03		2.5	2.75				

**Table S3:** FWHM (°C) of the derivative of the transmittance for Py<sub>n</sub>-PNIPAM solutions with a concentration of 0.5 g/L.

Heating Rate (°C/min)	Py <sub>1</sub> - PNIPAM (7K)	Py <sub>1</sub> - PNIPAM (12K)	Py <sub>1</sub> - PNIPAM (25K)	Py <sub>2</sub> - PNIPAM (7K)	Py <sub>2</sub> - PNIPAM (14K)	Py <sub>2</sub> - PNIPAM (26K)	Py <sub>2</sub> - PNIPAM (45K)
1.5	5.5	1.5	1	4	1.75	1.75	1
1	7	1.25	0.75	3.5	1.5	1.75	1
0.5	6.75	1.25	1	1.75	1.5	1.75	0.75
0.25	6.25	1.5	1.25	3	1.5	1.25	1

0.125	7.75	1	1	2.25	1.5	2	1.25
-------	------	---	---	------	-----	---	------

## Turbidimetry $T_c$ Results:

**Table S4:**  $T_c$  as determined by the peak in the derivative of % Transmittance for  $Py_n$ -PNIPAM solutions with a heating rate of 0.5 °C/min.

[Polymer] (g/L)	Py <sub>1</sub> - PNIPAM (7K)	Py <sub>1</sub> - PNIPAM (12K)	Py <sub>1</sub> - PNIPAM (25K)	Py <sub>2</sub> - PNIPAM (7K)	Py <sub>2</sub> - PNIPAM (14K)	Py <sub>2</sub> - PNIPAM (26K)	Py <sub>2</sub> - PNIPAM (45K)
1.0		29.75	30.75		21.25	27.25	29.75
0.5	30.25	30.25	31.5	21.5	23	28	30.25
0.25	32.25	30.75	32.25	23	24.25	29	30.75
0.15	34.5	31.75	32.5	24.25	25.75	29.5	31.25
0.1		32.25	33			29.75	31.5
0.03		33.75	34.5				

**Table S5:**  $T_c$  as determined by the peak in the derivative of % Transmittance for  $Py_n$ -PNIPAM solutions with a concentration of 0.5 g/L.

Heating Rate (°C/min)	Py <sub>1</sub> - PNIPAM (7K)	Py <sub>1</sub> - PNIPAM (12K)	Py <sub>1</sub> - PNIPAM (25K)	Py <sub>2</sub> - PNIPAM (7K)	Py <sub>2</sub> - PNIPAM (14K)	Py <sub>2</sub> - PNIPAM (26K)	Py <sub>2</sub> - PNIPAM (45K)
1.5	32.25	31.75	33.25	24	25	30	32
1	31.5	31	32.5	23.5	24.5	29	31.25
0.5	30.25	30.25	31.5	21.5	22.75	28	30.25
0.25	30.25	29.75	30.75	20.5	22.5	27.75	29.75
0.125	29	29.5	30.75	20	22.25	27.25	29.5



**Table S6:**  $T_c$  as determined by the intersection of the baseline and rise in the derivative of % Transmittance for Py<sub>n</sub>-PNIPAM solutions with a heating rate of 0.5 °C/min.

[Polymer] (g/L)	Py <sub>1</sub> - PNIPAM (7K)	Py <sub>1</sub> - PNIPAM (12K)	Py <sub>1</sub> - PNIPAM (25K)	Py <sub>2</sub> - PNIPAM (7K)	Py <sub>2</sub> - PNIPAM (14K)	Py <sub>2</sub> - PNIPAM (26K)	Py <sub>2</sub> - PNIPAM (45K)
1.0	21.25	29	30		19.75	25	28.52
0.5	24.52	29.25	30.5	19.25	21.25	27	29.25
0.25	28.25	29.25	30.75	22	22.75	28	30
0.15	31	29.75	31.25	22.25	24.5	28.25	30.25
0.1		29.52	31.5		27	28.75	30.5
0.03		32.25	32.5				31

**Table S7:**  $T_c$  as determined by the intersection of the baseline and rise in the derivative of % Transmittance for Py<sub>n</sub>-PNIPAM solutions with a concentration of 0.5 g/L.

Heating Rate (°C/min)	Py <sub>1</sub> - PNIPAM (7K)	Py <sub>1</sub> - PNIPAM (12K)	Py <sub>1</sub> - PNIPAM (25K)	Py <sub>2</sub> - PNIPAM (7K)	Py <sub>2</sub> - PNIPAM (14K)	Py <sub>2</sub> - PNIPAM (26K)	Py <sub>2</sub> - PNIPAM (45K)
1.5	26	30.5	32.25	21.27	23.25	28	30.75
1	25.5	29.75	31.25	20	22.25	27.25	30.25
0.5	23.75	29	30.5	19.25	21.25	26	29.25
0.25	23.25	28.5	30	18.75	20.5	25.25	28.25
0.125	23.25	28	29.75	18.5	20.25	24.75	27.5

## REFERENCES

1. Yip, J. Duhamel, J.; Qiu, X.-P. ; Winnik, F. M. Fluorescence Study of a Series of Monodisperse Telechelic  $\alpha,\omega$ -Dipyrenyl Poly(*N*-isopropylacrylamide)s in Ethanol and Water. *Can. J. Chem.* **2011**, *89*, 163-172.
2. Yip, J. Duhamel, J.; Qiu, X.-P. ; Winnik, F. M. Long-Range Polymer Chain Dynamics of Pyrene-Labelled Poly(*N*-isopropylacrylamide)s Studied by Fluorescence. *Macromolecules* **2011**, *44*, 5363-5372.